Transcriptome and Metabolome Integrated Analysis Reveals the mechanism of Cinnamomum bodinieri root response to alkali stress

Haozhang Han (21011@squ.edu.cn)
Suqian University
Lihua Zhang
Suqian University
Suhua Li
Suqian University
Rong Zhao
Suqian University
Fang Wang
Suqian University
Rong Dong
Suqian University
Xiaoli Wang
Suqian University

Research Article

Keywords: Cinnamomum bodinieri root, alkali stress, transcriptome, metabolome

Posted Date: January 20th, 2023

DOI: https://doi.org/10.21203/rs.3.rs-2487448/v1

Additional Declarations: No competing interests reported.

Version of Record: A version of this preprint was published at Plant Molecular Biology Reporter on April 6th, 2023. See the published version at https://doi.org/10.1007/s11105-023-01381-x.

Abstract

Cinnamomun bodinieri's normal growth and development are hampered by alkali stress, impeding its production and application of *Cinnamomum bodinieri*. The root organs being in direct contact with the cultivation environment, are sensitive to environmental stress. The present study revealed the differentially expressed genes and differentially metabolized products of *Cinnamomum bodinieri* root under alkali stress employing transcriptome and metabonomic analysis. The findings revealed that 690 differentially expressed genes and 269 metabolites were significantly different among HT6 and HCK6. Similarly, 1000 differentially expressed genes and 360 metabolites with significant differences were identified in HT48.vs.HCK48 combination. The combined analysis of transcriptome and metabolome identified 9 metabolic pathways at 6h and 48h after alkali treatment, including the biosynthesis pathway of tropane, piperidine and pyridine alkaloids, pyrimidine metabolic pathway, phenylalanine metabolic pathway, isoquinoline alkaloid biosynthesis pathway, glycolysis/gluconeogenesis pathway, flavonoid biosynthesis pathway, fatty acid biosynthesis pathway, carbon fixation pathway in photosynthetic organisms, the metabolic pathway of amino sugar and nucleotide sugar. Therefore, the strategy of *Cinnamomum bodinieri* to cope with alkali stress may be to increase osmotic regulation and antioxidant activity by accumulating alkaloids, flavonoids secondary metabolites, and N-acetyl-L-phenylalanine, ensure the stability of cell structure and function through the accumulation of lauric acid and palmitic acid, provide energy for plants to withstand alkali stress by accelerating the glycolysis process, and improve plants' resistance to biological and abiotic stress by inducing the activity of chitinase, The accumulation of oxaloacetic acid and other organic acids alleviates alkali stress environment. This study provides support for the analysis of the pathways and regulatory networks of *Cinnamomum bodinieri* in response to alkali stress.

1 Introduction

Soil salinization is a scourge for plant growth and crop yield. About 20% of the world's irrigated farmland is salinized to varying degrees, exceeding 7% of the earth's land area (Fang et al. 2021). China exhibits about 8.11×10^7ha saline alkali land area, accounting for 9% of China's land area. Human activities such as irrigation, fertilization, and global temperature rise lead to the expansion of salinization (Zhao et al. 2014). Alkaline soil accounts for the vast majority of salinized soil in the world. Alkaline soil is rich in Na^+, CO_3^{2-}, HCO_3^-, Cl^-, SO_4^{2-} plasma, and its pH value is often higher than 8.5 (José et al. 2002;Wang et al. 2021). The combined effects of ion toxicity, osmotic stress and high pH stress, make the alkaline saline soil more detrimental to plants (Aurelio et al. 2013; Zhou et al. 2022). There exist the knowledge gap in the current understanding on the alkali tolerance mechanism of plants,therefore the current study aim to bridge the gap by analyzing the pathways and regulatory networks of *Cinnamomum bodinieri* in response to alkali stress.

Direct involvement in exchange material and information with the cultivation environment, hails root system as main injured organ. It is known to all that a large number of metabolites are induced under alkali stress (Chu et al. 2019) as large amounts of small-molecule substances such as proline, soluble protein, betaine, sugar, polyols, and polyamines will be generated in sorghum seedlings (Sun et al. 2019). Similarly, it increases the the content of proline, soluble sugar, and polyol (sorbitol) in wheat (Guo et al. 2015). Moreover, the salt-tolerant perennial rhizome plant Leymus chinensis exhibit a higher concentration of nucleotides, amino acids, and organic acids, and a lower concentration of soluble sugars against alkali stress (Yan et al. 2022). The changes in the types and contents of these metabolites are generally considered necessary for plants to cope with alkali stress. Genetic and biochemical studies of rape in alkaline soil revealed an altered amino acid metabolic pathway and an increase in the expression of genes involved in potassium ion transport. The enhanced phenylalanine ammonia lyase (PAL) activity altered the biosynthetic pathway of other secondary metabolites and improved the tolerance of plants to alkali stress (Li et al. 2022). Citrus lateral root development is regulated by phytohormone pathway in response to alkali stress (Wu et al. 2019). Rice adapts to alkali stress through secondary metabolite biosynthesis, amino acid biosynthesis, iron homeostasis, diterpene, and phenylpropane biosynthesis (Li et al. 2020). Castor seeds regulate the osmotic balance and ROS level by promoting amino acid metabolism and the tricarboxylic acid cycle under alkali stress (Han et al. 2022). Vicia faba adapts to early alkaline salt stress by accumulating organic acids such as citric acid and malic acid (Sagervanshi et al. 2021).

Grapes rely on synthesizing organic acids such as oxalic acid and malic acid in root organs to respond to alkali stress (Xiang et al. 2019). Soybean responds to alkali stress by β-Oxidation, glycolysis, and tricarboxylic acid cycle (TCA cycle) (Zhang et al. 2016), while activating organic acid synthesis and maintaining intracellular ion and pH balance are the main strategies for wheat (Guo et al. 2017a). Similarly, energy metabolism and organic acid synthesis are the main ways for corn to respond to alkali stress (Guo et al. 2017b). It can be concluded that plant adaptation to alkali stress is a very nuanced process, and that various species of plants use a variety of responses to this environmental adversity. *Cinnamomun bodinieri*, an evergreen tree species and oil tree species of Cinnamomun in Lauraceae, is mainly distributed in Yunnan, Guizhou, western Hunan, eastern Sichuan, Hubei, and other regions of China. It likes acidic or slightly acidic soil and can grow poorly or even die because of the saline and alkaline cultivation environment in the seedling breeding and greening cultivation process. To analyze the pathways and regulatory networks of *Cinnamomun bodinieri* in response to alkali stress and provide important gene resources for the cultivation of new varieties resistant to alkali stress, it is necessary to study the mechanism of the root system of *Cinnamomun bodinieri* adapting to alkali stress.

2 Materials And Methods

2.1 Materials

The experiment was carried out in the seedling base of Suqian University. The seeds were collected from the same mother tree in August 2020, and sown in February 2021 after low-temperature stratification. The seedlings with normal growth and consistent growth height of 30 ± 2cm were selected as test materials in April 2022. The seedlings were cultured in a plastic hydroponic incubator (the volume of the nutrient solution was 38 L) with 1/2 Hoagland nutrient solution, during which the oxygen pump was used for 24h oxygenation. After 3 weeks of culture, Na_2CO_3 was added to the nutrient solution of each treatment, with a concentration of 0 (control) and 20mmol/L, respectively (when the concentration was higher than 20 mmol/L, the seedlings gradually died) based on the

previous observation. The pH of the nutrient solution after treatment was 7.50 and 9.50 respectively. At 6h and 48h after treatment, the fibrous roots of each treatment's seedlings were randomly sliced and frozen at -80℃ after liquid nitrogen quick freezing. Each treatment were performed in triplicates.

2.2 Transcriptome sequencing and analysis

2.2.1 Total RNA extraction, library construction, and sequencing

The total RNA of leaf materials was extracted using RNAperp Pure Plant Kit (Tiangen, Beijing) kit. The integrity of total RNA was detected by 1.2% agarose gel electrophoresis, whereas its purity and concentration were determined by the OD260/280 value of ultra micro nucleic acid protein analyzer(Nano-600, Shanghai Jiapeng). The cDNA library was constructed using EasyScript® One Step gDNA Removal and cDNA Synthesis SuperMix kit. The effective concentration of the library was accurately quantified by qRT-PCR followed by Illumina sequencing.

2.2.2 Functional annotation and enrichment analysis of differentially expressed genes.

The *Cinnamomum micranthum* genome was used as the reference for transcriptome analysis (https://www.ncbi.nlm.nih.gov/genome/57158). The clustering Unigene was annotated with KEGG (https://www.kegg.jp/kegg/pathway.html) and GO (http://www.geneontology.org/) databases. The differential analysis of gene expression was conducted with DESeq. The screening conditions of differentially expressed genes (DEGs) were P-value ≤ 0.05 and | log2Fold Changes | ≥ 1. When the value is greater than 1, the gene is identified as up-regulated expression. Otherwise, it is down-regulated expression.

2.2.3 Verification of differentially expressed genes

RT-PCR validated the screened genes for alkali tolerance in *Cinnamomum bodinieri*. The total RNA of the material was extracted with RNAperp Pure Plant Kit (Tiangen, Beijing, China). The genomic DNA was removed following PrimeScriptTM RT reagent Kit with gDNA Eraser (TaKaRa, Dalian, China) method. The cDNA product was generated by reverse transcription reaction with TR Prime Mix (random primer). Primers were designed in Primer 5.0 using Actin1 as the internal reference gene. The primer sequence has been listed (Table 1). A 20μL reaction volume system was prepared following the TransStart ® Green qPCR SuperMix kit method and amplified by Q2000B (Langji, Hangzhou, China) real-time fluorescence quantitative PCR instrument. The specific reaction system is as follows: 10μl 2×TransStart® Green qPCR SuperMix, 0.4μL Upstream/downstream primer (10μM) each, 1.5μL cDNA template, 7.7μL ddH_2O. The amplification conditions were as follows: pre-denaturation 94℃ 30s, amplification at 94℃ for 5s, and annealing at 60℃ for 30s, a total of 42 cycles. **Relative quantification** was done according to the $2^{-\Delta\Delta CT}$ method. Each sample was repeated 3 times. The primer was synthesized by Beijing Qingke Biotechnology.

Table 1
The primer sequence of the validated gene

Number	Gene	Forward primer (5' -3')	Reverse primer(5'-3')
1	*Actin1*	TAGTATGCCAGCGAACGAGT	TGCCATCTAGCTCCCTCTTG
2	C01311900	TACACGAGTGGGAAGCGAA	TCCAGCGGAAGATGAGACA
3	C00088500	CTGGGTAGCAGGTAAAAGC	GAAAGAGCGACAAGAGGAG
4	C00676500	GTAGTGGCTGAGTTGACGAA	GGAACAGTATCACCAAAAAAG
5	C01865600	ACTACTCCCGTTGCTGTTGA	AAGGATTCCCTGGGTTTATG
6	C01817700	GAGGTGTAGTGAGTGGGCTT	CATCTGTAATGTGGGGGAC
7	C00809200	CCACCAATCCTTCCTACTCT	CGTTCCCACTTCTGTCCTC
8	C00971400	ATGGAATGACAGAAGCAGGT	ATGGATGGCTAATGAGGAGA
9	C01147100	TCATCAATGCGAAGAAGACA	GAGAATCAGGATAGGCGACC

2.3 Metabolite extraction and metabolome analysis

2.3.1 Metabolite extraction

The material utilized was 40mg of sample ground with liquid nitrogen, which was combined with 200ML of ddH_2O and 800L of methanol/acetonitrile (V/V = 1:1). The samples were ultrasonically heated for 60min, static for 60min at -20℃, centrifuged at 16000g for 20min at 4℃. The supernatants were evaporated to dryness in a high-speed vacuum concentration centrifuge. The supernant was washed with 150ML acetonitrile-water solution (V/V = 1:1) and centrifuged at 16000g, 4℃ for 20min. All samples were mixed with 10μl of supernatant to form quality control samples (QC) for on-line detection.

2.3.2 Chromatographic separation

A High-performance liquid chromatography system (UHPLC, SHIMADZU-LC30) was employed for chromatographic separation using a HILIC column. The injector and column temperature was 4℃ and 25℃, respectively. The sample volume was 3μL, and the flow rate was set at 0.3 ml/min. The mobile phase A consisted of water and 25mmol/L ammonium acetate, and Phase B was acetonitrile. Chromatographic gradient elution procedure: 0 ~ 1min, 95% B; 1 ~ 7min, B changes linearly from 95–65%; 7 ~ 9min, B changes linearly from 65–35%; 9 ~ 10.5min, B maintained at 35%; 10.5 ~ 11min, B changes linearly from 35–95%; 11 ~ 15min, B is maintained at 95%.

2.3.3 Mass spectrum collection

The mass Thermo Scientific QE Plus was used for mass spectrometry analysis, and electric spray ionization (ESI) was used to identify the positive (+) and negative (-) ion modes. HESI source ionization settings: Spray Voltage: 3.8kv (+) and 3.2kv (-); Capillary Temperature: 320(±); Sheath Gas: 30(±); Aux Gas: 5(±); Probe Heater Temp: 350(±); S-Lens RF Level:50. Mass spectrum collection setting were as follows: the collection time was 12min; the scanning range of parent ion is 80 ~ 1200m/z, the resolution of primary mass spectrometry is 70000 @ m/z 200, AGC target: 3e6, and the primary Maximum IT: 100ms. Secondary mass spectrometry analyses were recorded using the following methods: after each full scan, trigger to collect the secondary mass spectrometry (MS2 scan) of 10 parent ions with the highest strength. Resolution of secondary mass spectrometry: 17500 @ m/z 200, AGC target: 1e5, secondary maximum IT: 50ms, MS2 Activation Type: HCD, Isolation window: 2m/z, Normalized fusion energy (Set ped): 10, 20, 30.

2.3.4 Data preprocessing and annotation

The MSDIAL software was used for peak alignment, retention time correction and peak integration extraction on the original data. The metabolite structure was identified by retrieving the HMDB public database and the standard metabolite library built by Shanghai Biotech Co., Ltd. through accurate mass number matching (mass tolerance < 20ppm) and secondary spectrum matching (mass tolerance < 0.02da). The ion peaks with the missing value (0 value) > 50% in the extracted data set were deleted, and the total peak area of the positive and negative ion data was normalized. Next, integrate the positive and negative ion peaks, apply R software for pattern recognition, and conduct subsequent data analysis after the data is preprocessed by Unit variance scaling (UV).

2.3.5 Data quality and stability verification

Two different strategies were picked to evaluate the system stability of this project: mass spectrum base peak chart comparison of QC samples and PCA statistical analysis of overall samples. Partial least square regression was used to establish the relationship model between the expression amount of metabolites and the sample category. Moreover, the prediction of the sample category was realized according to the variation between the predicted main component divisions on the PCA score map.

2.3.6 Differential metabolite screening and functional annotation

Metabolites with VIP > 1 and Pvalue < 0.05 were considered significantly different. The differential metabolites of each comparison group in the HMDB database were classified and counted, and the KEGG pathway enrichment analysis was performed.

2.4 Combined analysis of transcriptome and metabolome

R4.0.1-win and Cytoscape 3.8.2 software was employed for transcription metabolism joint analysis of KEGG metabolic pathways and identified the common KEGG metabolic pathway between HCK6.V.HT6 and HCK48.V.HT48 after 6h and 48h of alkali treatment.

3 Results And Analysis

3.1 Transcriptome analysis

3.1.1 Statistical analysis of transcriptome data

Four root samples of Cinnamomum bodinieri were subjected to RNA seq analysis after exposure to alkali stress for 6 and 48 hours, and all transcriptome data were stored in NCBI (https://dataview.ncbi.nlm.nih.gov/object/PRJNA923153?reviewer=qkp854043qvct67nbukvepfns1). PCA showed low variability between biological duplicate samples, indicating a high correlation between duplicate samples (Fig. 1A). Pearson correlation analysis of gene expression levels revealed the correlation coefficient ranging from 0.8 to 1 (Fig. 1B), indicating an enhanced correlation between samples. The 12 cDNA libraries constructed (the control and treatment of alkali stress for 6h and 48h) produced 6.57-8.35G base data (Table 2), in which the percentage of Q30 (the percentage of sequences with sequencing error rate < 0.1%) ranged from 92.79–93.57%. The percentage of fuzzy bases ranged from 0.000293–0.00031%. Cinnamomum camphora was used as the reference genome for alignment (Table 3), and the total number of sequences used for alignment was 39984454 ~ 49986432. The percentage of sequences aligned to the reference genome, multiple location and single location was 84.49%~87.74%, 5.47%~17.05%, and 82.95%~94.53%, respectively. The abovementioned findings signify that RNA seq is good quality and suitable for future investigation.

Table 2
Transcriptome sequencing quality

Sample	Reads No.	Bases (bp)	Q30 (bp)	N (%)	Q20 (%)	Q30 (%)
HCK61	46789192	7065167992	6561789146	0.000295	97.25	92.87
HCK62	47101250	7112288750	6612002543	0.000306	97.25	92.96
HCK63	50233922	7585322222	7057261229	0.000296	97.31	93.03
HT61	55283062	8347742362	7775037651	0.00031	97.29	93.13
HT62	43558080	6577270080	6154425245	0.000295	97.55	93.57
HT63	51597560	7791231560	7275265950	0.000305	97.5	93.37
HCK481	43736676	6604238076	6149451430	0.000307	97.36	93.11
HCK482	46806648	7067803848	6569079274	0.000299	97.31	92.94
HCK483	45831040	6920487040	6421712826	0.000293	97.22	92.79
HT481	48193306	7277189206	6789621722	0.000309	97.39	93.3
HT482	44821560	6768055560	6304784183	0.000303	97.38	93.15
HT483	47150486	7119723386	6619525885	0.000294	97.3	92.97

Table 3
RNASeq Map Statistics

Sample	Clean_Reads	Total_Mapped	Multiple_Mapped	Uniquely_Mapped
HCK61	42980984	36884178 (85.82%)	3565262 (9.67%)	33318916 (90.33%)
HCK62	43358150	36707255 (84.66%)	2714425 (7.39%)	33992830 (92.61%)
HCK63	46445098	40275459 (86.72%)	6267397 (15.56%)	34008062 (84.44%)
HT61	49986432	43859970 (87.74%)	7476417 (17.05%)	36383553 (82.95%)
HT62	39984454	34975926 (87.47%)	3856175 (11.03%)	31119751 (88.97%)
HT63	47131564	40124837 (85.13%)	2618490 (6.53%)	37506347 (93.47%)
HCK481	39959500	34156911 (85.48%)	2331747 (6.83%)	31825164 (93.17%)
HCK482	42809888	36170213 (84.49%)	1979400 (5.47%)	34190813 (94.53%)
HCK483	41757968	36200399 (86.69%)	2315877 (6.40%)	33884522 (93.60%)
HT481	43346384	36629699 (84.50%)	2257402 (6.16%)	34372297 (93.84%)
HT482	41154116	35128985 (85.36%)	2709833 (7.71%)	32419152 (92.29%)
HT483	42855304	36524511 (85.23%)	2717064 (7.44%)	33807447 (92.56%)

3.1.2 Expression difference analysis

Over the course of 6 hours of alkali stress, 418 genes were up-regulated, 272 genes were down-regulated, and 24117 genes were not differently expressed. (Fig. 3A). Similarly, at 48h of alkali stress, 492 genes were identified to be up-regulated, 508 genes to be down-regulated, and 23865 genes to be non-differentially expressed (Fig. 3B). Two-way cluster analysis revealed the identical number of DEGs across groups. Still, there exristed huge difference between groups at the same treatment period, and the difference between groups at different treatment times is even more significant (Fig. 3C). The common DEGs of HT6.V.HCK6 and HT48.V.HCK48 combinations under alkali stress for 6h and 48h were observed to be 120, the unique DEGs in HT6.V.HCK6 and HT48.V.HCK48 combination were observed to be 570 and 880, respectively (Fig. 3D).

3.1.3 GO analysis and KEGG enrichment analysis

The findings revealed that the DEGs of *Cinnamomun bodinieri* roots in HT6.V.HCK6 combination are mainly enriched in terms such as the biosynthesis process of active oxygen species, active nitrogen metabolism, oxidoreductase activity acting on other nitrogen oxides, reductase activity, nitrogen cycle metabolism, nitric oxide metabolism, nitric oxide biosynthesis, nitrate reductase [NAD(P)H] activity, nitrate metabolism, nitrate assimilation Neurotransmitter biosynthesis process, molybdenum polypeptide cofactor binding, molybdenum ion binding, cell phosphate ion dynamic balance, cell monovalent inorganic anion dynamic balance, cell anion dynamic balance, catalytic activity. Similarly, the differentially expressed genes of *Cinnamomun bodinieri* root in HT48.V.HCK48 combination are mainly enriched in the reactions to boron containing substances, biological stimuli, adenosine phosphate sulfate reductase (thioredoxin), negative regulation of protein metabolism, negative regulation of peptidase activity, negative regulation of molecular function, negative regulation of cell protein metabolism, negative regulation of catalytic activity, horizontal plasma membrane function, fruit ripening, flavonoids metabolism,

development and maturity Defense reaction, cysteine-type endopeptidase inhibitor activity, catalytic activity, lysosome-related organelle biogenetic complex, arsenite transport, arsenite transmembrane transport protein activity, and mature anatomical structure.

According to the KEGG pathways enrichment analysis, the DEGs of *Cinnamomun bodinieri* roots in HT6.V.HCK6 combination were mainly enriched pathways including folic acid biosynthesis, plant hormone signal transduction, glutathione metabolism, photosynthesis, nicotinic acid and nicotinamide metabolism, mutual transformation of pentose and glucosidic acid, biotin metabolism, caffeine metabolism, fructose and mannose metabolism, flavonoids and flavonol biosynthesis, cyano amino acid metabolism, thiometabolism, ABC transporter, MAPK signal pathway – plant, phenylpropane biosynthesis, nitrogen metabolism, isoquinoline alkaloid biosynthesis, tyrosine metabolism, sesquiterpene and triterpene biosynthesis, plant – pathogen interaction. Moreover, The DEGs of *Cinnamomun bodinieri* root in HT48.V.HCK48 combination were mainly enriched in pathways includings nitrogen metabolism, carotenoid biosynthesis, starch and sucrose metabolism, AGE RAGE signaling pathway, thiometabolism β – Alanine metabolism, cyanide metabolism, biosynthesis of stilbenes, diarylheptane and gingerol, flavonoids biosynthesis, cutin, aberdeen and wax biosynthesis, anisodane, piperidine and pyridine alkaloids biosynthesis, tyrosine metabolism, monoterpene biosynthesis, cysteine and methionine metabolism, isoquinoline alkaloids biosynthesis, glutathione metabolism, phenylalanine metabolism, diterpene biosynthesis Phenylpropane biosynthesis, plant pathogen interaction.

3.1.4 Verification of differential gene expression

Cinnamomum bodinieri's alkaline stress resistance KEGG genes were picked and performed real-time fluorescence quantitative PCR to verify the reliability of transcriptome data. The qRT-PCR data were compared with transcriptome data, as shown in Fig. 5. The Pearson correlation analysis shows that the qRT-PCR results were significantly correlated with the transcriptome sequencing results at 0.05. The expression trend of the selected genes is consistent, indicating that this study's RNA sequencing results are relatively reliable.

3.2 Analysis of metabolome

3.2.1 Differential metabolite screening

Root and QC samples of Cinnamomum bodinieri were analyzed using principal component analysis After 6h and 48h of alkali treatment. QC samples were clustered closely, indicating that this project's experiment's repeatability was good (Fig. 6-A; Fig. 6-B). After 6 h alkali stress, 269 secondary metabolites with a significant difference were screened from HT6. vs. HCK6 group, including 175 up-regulated and 94 down-regulated metabolites. A total of 360 secondary metabolites with significant differences were screened from HT48.vs.HCK48 group, including 201 up-regulated and 159 down-regulated after 48h of alkali stress treatment (Fig. 6-C). Wayne diagram analysis revealed that 194 metabolites were identified in both combinations (Fig. 6-D). After 48h alkali treatment, the number of secondary metabolites with significant difference increased by 91 compared with 6h alkali treatment, of which 26 were up-regulated, and 65 were down-regulated.

3.2.2 Differential metabolite classification and KEGG analysis

The findings of KEGG and HMDB classification of differential metabolites revealed that the differential metabolites identified in HT6.V.HCK6 combination mainly include five KEGG classifications: alkaloids, fatty acids, nucleic acids, polyketones, and terpenoids, with four HMDB classifications: lipid and lipoid molecules, nucleosides, nucleotides and analogs, organic acids and derivatives, organic heterocyclic compounds, phenylpropanes, and polyketones (Fig. 7-A). The differential metabolites identified in HT48.V.HCK48 combination mainly include 7 KEGG classifications of alkaloids, carbohydrates, nucleic acids, polyketones, sterol lipids, sterols and terpenoids, whereas eight HMDB classifications: alkaloids and their derivatives, benzene compounds, lipids and lipid molecules, nucleosides, nucleotides and analogs, organic acids and their derivatives, organic oxygen compounds, organic heterocyclic compounds, phenylpropanes and polyketones (Fig. 7-B). in addition, the KEGG pathway enrichment analysis revealed the zeatin biosynthesis pathway and pyrimidine metabolism pathway among the 30 KEGG pathways enriched in HT6.V.HCK6 combination are significant (Fig. 8-A). Among the 30 KEGG pathways enriched after 48h alkali treatment, the aldosterone synthesis and secretion pathway, bile secretion, cortisol synthesis and secretion, progesterone mediated oocyte maturation, flavonoid biosynthesis, pyrimidine metabolism, Cushing's syndrome, insulin resistance, oocyte meiosis pathways are more significant (Fig. 8-B).

3.3 Combined analysis of transcriptome and metabolome

Metabolite proteins that varied significantly across the metabolic and transcriptional groups were analyzed using the KEGG. The KEGG pathway in each group was compared, and a Venn diagram was drawn. The differential metabolites in the HT6.V.HCK6 combination were enriched in 174 KEGG pathways, the metabolic proteins of DEGs were enriched in 79 KEGG pathways, and 34 KEGG pathways were enriched in both of them (Fig. 9-A). The differential metabolite of HT48.V.HCK48 combination enriched 182 KEGG pathways, whereas the metabolic protein of differential expression genes enriched 77 KEGG pathways, and 35 KEGG pathways were enriched by both (Fig. 9-C). The KEGG pathway enriched in both metabolome and transcriptome was analyzed, and these significant KEGG pheat map were plotted. According to the joint analysis results of transcriptome and metabolome, the KEGGs co-enriched in HT6.V.HCK6 combination include sesquiterpene and triterpene biosynthesis, phenylpropane biosynthesis, ABC transporter, isoquinoline alkaloid biosynthesis, tyrosine metabolism, pyrimidine metabolism, glycolysis/gluconeogenesis, phenylalanine metabolism, carbon fixation in photosynthetic organisms, fatty acid biosynthesis, flavonoid biosynthesis, metabolism of amino sugar and nucleotide sugar, biosynthesis of tropane, piperidine and pyridine alkaloids (Fig. 9-B). Significant KEGGs co-enriched in HT48.V.HCK48 combination include flavonoids biosynthesis, scopolamine, piperidine, and pyridine alkaloids biosynthesis, pyrimidine metabolism, carbon fixation in photosynthetic organisms, glycolysis/gluconeogenesis, nicotinic acid, and nicotinamide metabolism, fatty acid biosynthesis, alanine, aspartic acid, and glutamic acid metabolism, galactose metabolism, zeatin biosynthesis, an amino sugar, and nucleotide sugar metabolism, diterpene and cutin biosynthesis, aberine and wax, an isoquinoline alkaloid, phenylalanine metabolism, and glutathione metabolism.

Table 4
Differential expression genes and metabolites related to alkali stress in HT6.V.HCK6 combination

Number	PathwayID	KEGG	DEGS		Differential metabolites
			up-regulated	down-regulated	up-regulated
1	ko00941	Flavonoid biosynthesis	C00840400,C00663500	/	/
2	ko00960	Tropane, piperidine, and pyridine alkaloid biosynthesis	C01311900	C01984800	Senecionine;Scopolamine
3	ko00240	Pyrimidine metabolism	/	C00083800,C00088500	Uridine 5'-diphosphate(UDP);Uridine;Uracil;Malonic acid
4	ko00710	Carbon fixation in photosynthetic organisms	C02571800	C01828900	Oxaloacetic acid
5	ko00010	Glycolysis / Gluconeogenesis	C00676500,C01901700	/	Oxaloacetic acid
6	ko00950	Isoquinoline alkaloid biosynthesis	C02513300,C01470700,C01331000, C01470800,C01981800	C01984800	Corydaline
7	ko00061	Fatty acid biosynthesis	C00596200,C01426300,C01026300	/	Malonic acid; Lauric acid;Palmitic acid
8	ko00360	Phenylalanine metabolism	C00663500	C01984800	N-Acetyl-L-phenylalanine
9	ko00520	Amino sugar and nucleotide sugar metabolism	C02314100,C02024400,C00676500, C01970400	C01511900	N-Acetylmuramic acid

Table 4
Differential expression genes and metabolites related to alkali stress in HT48.V.HCK48 combination

Number	PathwayID	KEGG	DEGS		Differential metabolites
			up-regulated	down-regulated	up-regulated
1	ko00941	Flavonoid biosynthesis	C02738500,C00777600,C02419100	C00446100,C01147100	Afzelechin;Quercetin; Homoeriodictyol
2	ko00960	Tropane, piperidine, and pyridine alkaloid biosynthesis	C01865600,C00621500	C01984800,C02644300,C01648100	Senecionine;Scopolamine
3	ko00240	Pyrimidine metabolism	/	C01817700,C00083800,C01969900	Uridine 5'-diphosphate;Deoxythymidine
4	ko00710	Carbon fixation in photosynthetic organisms	C01523600,C00179500,C01580800, C01523700	C02293100	Oxaloacetic acid
5	ko00010	Glycolysis / Gluconeogenesis	C01523700,C01523600,C00435300	/	Oxaloacetic acid
6	ko00950	Isoquinoline alkaloid biosynthesis	C01112900,C02513300,C00621500, C01865600	C01648100,C02644300,C01984800	Lycorine;Corydaline
7	ko00061	Fatty acid biosynthesis	C00596200,C02303300	/	Lauric acid;Palmitic acid;Stearic acid
8	ko00360	Phenylalanine metabolism	C00971400,C01865600,C00621500	C02644300,C01648100,C01984800, C00809200,C01147100	N-Acetyl-L-phenylalanine
9	ko00520	Amino sugar and nucleotide sugar metabolism	C01970200	C02588600,C00317500,C00317400, C02620600	/

Note: "/" in the table indicates that relevant differentially expressed genes or differentially expressed metabolites cannot be identified.

4 Conclusion And Discussion

Mir et al. (2018) found that jasmonic acid enhanced plant redox status in response to alkaline stress by regulating proline and glutathione metabolic pathways. Lignosulfonic acid and polyacrylamide can regulate osmotic pressure and antioxidant system under saline-alkali stress by up-regulating phenylpropane biosynthesis pathway, up-regulating the K^+transport gene and K^+/Na^+ratio in plant leaves (An et al. 2020; Li et al. 2022). After being exposed to alkali for 6 hours, the roots of *Cinnamomum bodinieri* showed a significant increase in the expression of genes and metabolites, as determined by transcriptome and metabolome analyses. Roots of *Cinnamomun bodinieri*, after 48h exposure to alkali stress, hampered the gene and metabolite up-regulation. It is indicating that *Cinnamomum bodinieri* tree actively responds to alkali stress by increasing nutrient absorption after 6h of alkali treatment, and its root growth and development are affected after 48h of alkali treatment, mainly through protein function and secondary metabolism to mitigate alkali stress. According to the combined analysis results of transcriptome and metabolome, the biosynthesis of tropane, piperidine, and pyridine alkaloids, isoquinoline alkaloids, pyrimidine metabolism, phenylalanine metabolism, glycolysis/gluconeogenesis, flavonoid biosynthesis, fatty acid biosynthesis, carbon fixation in photosynthates, amino sugar and nucleotide sugar metabolic pathways were significantly enriched at 6h and 48h of alkali treatment, which may participate in the alkali tolerance of *Cinnamomum bodinieri*.

Senecine and scopolamine were considerably up-regulated, and piperine downregulated in the synthesis pathway of tropine, piperidine, and pyridine alkaloids after 6h and 48h of alkali treatment, respectively (Table 4 and Table 5). HT6.vs.HCK6 and HT48.vs.HCK48 combination transcriptome analysis identified that the expression of C01311900 gene and C01865600, C00621500 was significantly up-regulated. Blast comparison results showed that C01311900, C01865600 and C00621500 encodes tropine reductase (TR), tyrosine aminotransferase, and primary amine oxidase (AOC), respectively. All of which are involved in the synthesis of scopolamine. At 6h and 48h of alkali treatment, Corydalis exhibited significantly increased expression in the isoquinoline alkaloid biosynthesis pathway, whereas codeine and colchicine exhibited significant;y decreased expression. Transcription group analysis showed that the gene expression of C02513300, C01470700, C01331000, C01470800, and C01981800 was significantly up-regulated in HT6.vs.HCK6 combination transcriptome analysis. HT48.vs significantly up-regulated the gene expression of C01112900, C02513300, C00621500 and C01865600.HCK48 combination transcriptome analysis. Blast comparison findings revealed that C01470700 and C01470800 encode tyrosine decarboxylase. At the same time, C01112900, C02513300, C01331000, and C01981800 code for polyphenol oxidase, and C01865600 and C00621500 code for primary amine oxidase, both of which are involved in the synthesis of Corydalis. It can be inferred that the accumulation of scopolamine and Corydalis is involved in the alkali-resistant process of *Cinnamomum bodinieri*, which may be related to its antioxidant activity (Jia et al. 2019).At 6h and 48h of alkali treatment, UDP expression was significantly up-regulated in the pyrimidine metabolic pathway. Transcription group analysis of HT6.vs.HCK6 combination identified that C00083800 and C00088500 gene expression was downregulated, while HT48. vs.HCK48 combination identified that C01817700, C00083800 and C01969900 gene expression was down regulated. Blast comparison results showed that C00083800 encodes uridine triphosphate pyrophosphate hydrolase, C00088500 encodes uridine 5'- monophosphate ribose hydrolase, C01817700 encodes CTP synthase, and C01969900 encodes uridine 5' - monophosphate ribose hydrolase. Downregulation of these genes reduces UDP consumption. UDP may participate in synthesizing glycosyl donors to promote the glycosylation process of flavonoids (Li et al. 2016; Mashima et al. 2019). At 6h and 48h of alkali treatment, the metabonomic analysis identified that the expression of oxaloacetic acid was up-regulated, and the expression of salicin was downregulated in the glycolysis/gluconeogenesis pathway. HT6.vs.HCK6 combination transcriptome analysis identified that C00676500 and C01901700 genes were up-regulated. According to Blast comparison results, C00676500 encodes hexokinase and participates in the process of glucose-forming pyruvate during glycolysis. C01901700 encodes alcohol dehydrogenase (ADH), which is involved in the regeneration of NAD^+ so that glycolysis can continue (Noguchi et al. 2007; So et al. 2017); HT48.vs.HCK48 combination transcriptome analysis up-regulated the expression of C01523700, C01523600, and C00435300. Blast comparison results revealed that C01523700 and C01523600 encode phosphoglycerate kinase, C00435300 encodes phosphoglycerate mutase, participates in forming phosphoenolpyruvate, and accumulates oxaloacetic acid through the catalysis of phosphoenolpyruvate carboxylase during glycolysis. In addition to participating in osmotic regulation and maintaining glycolysis, oxaloacetate accumulation can also participate in the pH regulation process. For example, alkali stress increases phosphoenolpyruvate carboxylase activity in grape roots, catalyzes the carboxylation of phosphoenolpyruvate bicarbonate oxaloacetate, and then converts it into oxalic acid and malic acid (Xiang et al. 2019), to conduct pH regulation. At 6h and 48h of alkali treatment, the metabonomic analysis identified that the expression of oxaloacetate was up-regulated, and the expression of 5-ribophosphate was downregulated in the carbon assimilation pathway of photosynthetic organisms. The transcriptome analysis of HT6.vs.HCK6 combination identified that the expression of the C02571800 gene was up-regulated, and the expression of C01580800, C01523600, C01523700, and C00179500 was up-regulated in HT48.vs.HCK48 combination. The Blast comparison results indicate that C02571800 encodes phosphoenolpyruvate carboxylase, which can catalyze the reaction of phosphoenolpyruvate with CO_2 molecules to form oxaloacetic acid and promote the accumulation of oxaloacetic acid. C01580800 encodes glyceraldehyde-3-phosphate dehydrogenase, which catalyzes D-glyceraldehyde-3-phosphate to form 1,3-diphospho-D-glycerate. C01523600 and C01523700 encode phosphoglycerate kinase, which catalyzes 1,3-diphospho-D-glycerate to form 3-phosphate-D-glycerate and ATP, accelerating glycolysis. C00179500 encodes NADP-dependent malic enzyme, catalyzes the conversion of (S)-malic acid to pyruvate, and reduces $NADP^+$ to NADPH, releasing H^+, which plays an important role in stabilizing the cytoplasm pH and maintaining the balance of ion absorption by plant roots (Drincovich et al. 2001; Chen et al. 2019; Badia et al. 2020). N-acetyl-L-phenylalanine was shown to have its expression increased after 6h and 48h of alkali treatment, whereas phenylacetaldehyde's expression decreased throughout the phenylalanine metabolic pathway. The expression of C00663500 was up-regulated by transcriptome analysis of HT6.vs.HT48.vs up-regulated the HCK6 combination and the expression of C01865600, C00621500, and C00971400.HCK48 combination; According to Blast comparison results, C00663500 encodes caffeoyl CoA O-methyltransferase (CCo AOMT), which can catalyze caffeoyl CoA to form ferulic CoA and is a key enzyme for lignin synthesis (Day et al. 2009). C01865600 and C00621500 encode primary amine oxidase, which catalyzes phenylacetaldehyde to absorb hydrogen peroxide to form phenylethylamine and promotes the accumulation of N-acetyl-L-phenylalanine. Under alkaline stress, N-acetyl-l-phenylalanine mainly acts through osmotic stress (Li et al. 2022) and antioxidant stress. In addition, in the phenylalanine metabolic pathway, C00809200 encodes phenylalanine ammonia lyase, C01147100 encodes caffeoyl CoA-O-methyltransferase, and C00971400 encodes 4-coumaric acid CoA ligase (4CL), which are the key enzymes in the phenylalanine biosynthesis of lignin monomers, plant hormones, flavonoids, and phenylalanines. 4CL is divided into two categories, among which class I is involved in the synthesis of lignin monomers, and class II is mainly involved in the enzymatic reaction of flavonoids synthesis (Lavhale et al.

2018; Xiong et al. 2019). The expression of C01147100 and C00809200 in the HT48.V.HCK48 combination was downregulated, while C00971400 was upregulated. It was speculated that coumarinyl CoA was mainly involved in the downstream flavonoid metabolism pathway at the later stage of alkali stress. Flavonoids have been proven to participate in plants' abiotic stress process. The transcriptome analysis of HT6. vs.HCK6 combination identified that the flavonoid biosynthesis pathway C00840400 and C00663500 genes were up-regulated. According to the Blast comparison results, C00840400 encodes 5-O-(4-coumoyl)-D-quinic acid 3 '-monooxygenase (CYP98A, C3'H), which is involved in the synthesis of caffeoyl CoA. C00663500 encodes caffeoyl CoAO methyltransferase, which can synthesize caffeoyl CoA into ferulic CoA, but the metabonomic analysis did not detect the up-regulated expression of related metabolites. The metabolomic analysis of HT48. vs. HCK48 combination noted that the expression of catechin, quercetin, and hallucinogens in the flavonoid biosynthesis pathway was significantly up-regulated. The transcriptome analysis of HT48.vs.HCK48 combination identified that the expression of C02738500, C02419100, and C00777600 was up-regulated, and the expression of C00446100 and C01147100 was downregulated. According to the Blast comparison results, C02738500 and C02419100 encode shikimic acid O-hydroxycinnamoyltransferase (HCT), which can promote the formation of caffeic CoA and shikimic acid from 5-O-caffeic acid shikimic acid. C01147100 encodes caffeoyl coenzyme A O-methyltransferase, whose expression is downregulated, which inhibits the formation of ferulic coenzyme A from caffeoyl CoA. It promotes the formation of (2S)-naringen and (2S)-sage grass phenol. C00777600 is a flavanone 3-hydroxylase F3H, which is mainly involved in forming avermectin, quercetin, and kaempferol in the flavonoids biosynthesis pathway with (2S)-naringenin and (2S)-kaempferol as the substrate. However, avermectin, quercetin, and kaempferol have been proven to have high antioxidant activity, and flavonoids may participate in the alkali stress resistance process of *Cinnamomum bodinieri* through antioxidant activity (Xu et al. 2020). The expression of malonic acid, lauric acid, and palmitic acid in fatty acid metabolism-related pathways of HT6. vs. HCK6 combination was significantly up-regulated, while the expression of palmitic acid, lauric acid, and stearic acid in HT48.vs.HCK48 combination was significantly up-regulated. The transcriptome analysis of HT6. vs. HCK6 combination identified that C00596200, C01426300 and C01026300 genes were up-regulated. According to the Blast comparison result, C01426300 code β-Ketoacyl acyl carrier protein reductase is involved in forming lauroyl-(acyl carrier protein) and palmitoyl-(acyl carrier protein) from malonic acid. C01026300 encodes lauroyl acyl carrier protein hydrolase, which can convert lauroyl-(acyl carrier protein) to lauric acid; C00596200 encodes palmitoyl acyl carrier protein thioesterase, which can convert palmitoyl-(acyl carrier protein) to palmitic acid. The transcriptome analysis of HT48.vs.HCK48 combination identified that the expression of C00596200 and C02303300 was up-regulated. The Blast comparison findings revealed that C02303300 encodes palmitoyl coenzyme A synthase, which can synthesize palmitic acid into palmitoyl coenzyme A, and palmitoyl coenzyme A is involved in the metabolism of glyceride or glycerol phospholipid, thereby promoting the stability and signal transduction of biofilm (Aurelio et al. 2013; Ritter et al. 2014).The metabonomic analysis of HT6.vs.HCK6 combination identified that the expression of N-acetyl cytosolic acid was up-regulated, and the expression of N-acetylneuraminic acid, UDP-D-xylose, and UDP glucose was downregulated in the metabolism of amino sugar and nucleotide sugar. HT48. vs.HCK48 combination identified the expression of UDP-N-acetylglucosamine, N-acetylneuraminic acid, D-glucosamine phosphate, UDP-D-xylose, and UDP glucose was downregulated. The transcriptome analysis of HT6.vs.HCK6 combination identified that C02024400, C01970400, C02314100, and C00676500 genes were up-regulated. According to Blast comparison results, C02024400 and C01970400 encode chitinase, which can catalyze chitin β-Hydrolysis of the 1,4-glycosidic bond to produce N-acetylamine glucose oligomer or N-acetyl-β-D-glucosamine monomer, C00676500 encodes hexokinase, C02314100 encodes mannose-6-phosphate isomerase, which is jointly involved in the process of chitin decomposition to form N-acetyl muriatic acid, improving plant biological and abiotic resistance (Ahmed et al. 2012; Mir et al. 2020). The transcriptome analysis of HT48.vs.HCK48 combination identified that only the expression of the C01970200 gene encoding chitinase was up-regulated, and the plant resistance was decreased.

In summary, root tissue adaptation strategies to alkali stress environments differ from those of other plants. According to the joint analysis results of transcriptome and metabolome, the biosynthesis of tropane, piperidine, and pyridine alkaloids, isoquinoline alkaloids, pyrimidine metabolism, phenylalanine metabolism, glycolysis/gluconeogenesis, flavonoid biosynthesis, fatty acid biosynthesis, carbon fixation in photosynthetic organisms, and the metabolic pathways of amino sugar and nucleotide sugar is related to the adaptation of *Cinnamomum bodinieri* to alkali stress; The accumulation of the critical metabolites scopolamine, Corydalis, UDP, N-acetyl-L-phenylalanine, oxaloacetic acid, alfcatechin, quercetin, hallowanin, lauric acid, palmitic acid and N-acetyl muriatic acid cooperatively participated in the alkali resistant response process of *Cinnamomum bodinieri*. The strategy of *Cinnamomum bodinieri* to cope with alkali stress may be to increase osmotic regulation and antioxidant activity by accumulating alkaloids, flavonoids secondary metabolites, and N-acetyl-L-phenylalanine, ensure the stability of cell structure and function through the accumulation of lauric acid and palmitic acid, provide energy for plants to withstand alkali stress by accelerating the process of glycolysis, and improve plants' resistance to biological and abiotic stress by inducing the activity of chitinase, The accumulation of oxaloacetic acid and other organic acids may alleviate alkali stress environment.

Declarations

Ethical Approval

This manuscript is not applicable for both human and/ or animal studies.

Competing interests

The authors declare that they have no known competing financial interests or personal relationships that could have appeared to influence the work reported in this paper.

Authors' contributions

HHZ conceived the idea,and ZLH performed the experiments; ZLH, LSH and ZR analyzed the data; HHZ and ZLH wrote the manuscript. WF , DR and WXL constructed and improved the figures. All authors have read and approved the final version of the manuscript.

Funding

This project is jointly funded by the Natural Science Foundation of Jiangsu Province (BK20201481), the Suqian Science and Technology Program (M202001), the Suqian Science and Technology Program (L202004), and the Suqian University Innovation Team Project (2021td05).

Availability of data and materials

All data generated or analysed during this study are included in this published article (and its supplementary information files).

References

1. Ahmed NU, Park JI, Jung HJ, et al(2012)Molecular characterization of stress resistance- related chitinase genes of Brassica rapa. Plant physiology and biochemistry.58:106–115.
2. An M, Wang X, Chang D, et al(2020)Application of compound material alleviates saline and alkaline stress in cotton leaves through regulation of the transcriptome. BMC Plant Biol. https://doi:10.21203/rs.3.rs-31407/v2
3. Aurelio GC,Carlos de O,Matías M,et al(2013)Metabolomics as a tool to investigate abiotic stress tolerance in plants. International Journal of Molecular Sciences.14 (3): 4885–4911.
4. Badia MB, Maurino VG, Pavlovic T, et al(2020)Loss of function of Arabidopsis ADP-malic enzyme 1 results in enhanced tolerance to aluminum stress. The Plant Journal.101 (3):653–665.
5. Chen QQ, Wand BP,Dinu HY, et al(2019)Review: The role of NADP-malic enzyme in plants under stress. Plant Science.281:206–212.
6. Chu LL,Luo CK,Tian L, et al(2019)Research advance in plants*0* adaptation to alkali stress. J. Plant Genet. Resour. *20*, 836–844.
7. Day A, Neutelings G, Nolin F, et al(2009)Caffeoyl coenzyme A O-methyltransferase down-regulation is associated with modifications in lignin and cell-wall architecture in flax secondary xylem[J]. Plant Physiology & Biochemistry, 2009, 47(1): 9–19.
8. Drincovich MF, Casati P, Andreo CS(2001)NADP-malic enzyme from plants: a ubiquitous enzyme involved in different metabolic pathways. FEBS Letters. 490:1–6.
9. Fang S, Hou X, and Liang X (2021) Response mechanisms of plants under saline-alkali stress. Front Plant Sci. https://doi.org/10.3389/fpls.2021.667458.
10. Guo R, Yang Z, Li F, et al (2015) Comparative metabolic responses and adaptive strategies of wheat (*Triticum aestivum*) to salt and alkali stress. BMC Plant Biol. https://doi.org/10.1186/s12870-015-0546-x
11. Guo R,Zhou J,Yang F,et al(2017a)Effects of alkaline stress on metabonomic responses of wheat (*Triticum aestivum* Linn) leaves. Sci. Agric. Sin.*50*:250–259.
12. Guo R,Shi LX,Yan CR,et al(2017b)Ionomic and metabolic responses to neutral salt or alkaline salt stresses in maize (*Zea mays* L.) seedlings. BMC Plant Biol.https://doi.org/10.1186/s12870-017-0994-6
13. Han PL,Li SX,Yao KS,et al(2022)Integrated metabolomic and transcriptomic strategies to reveal adaptive mechanisms in castor plant during germination stage under alkali stress. Environmental and Experimental Botany.https://doi.org/10.1016/J.ENVEXPBOT.2022.105031
14. Jia XM, Zhu YF, Hu Y,et al(2019)Integrated physiologic, proteomic, and metabolomic analyses of Malus halliana adaptation to saline–alkali stress. Horticulture Research. https://doi.org/10.1038/s41438-019-0172-0
15. José GA,Ildefonso PS and Rafael C(2002) A model to explain high values of pH in an alkali sodic soil Modelo para explicar valores elevados de pH em um solo sódico alcalino. Scientia Agricola,59(4): 763–770.
16. Lavhale SG,Kalunke RM,Giri AP(2018)Structural,functional and evolutionary diversity of 4-coumarate-Co A ligase in plants.Planta.248(5):1063–1078.
17. Li LN, Kong JQ(2016)Transcriptome-wide identification of sucrose synthase genes in Ornithogalum caudatum. Rsc Advances,6(23):18778–18792.
18. Li Q,Ma CK,Tai HH,et al(2020)Comparative transcriptome analysis of two rice genotypes differing in their tolerance to saline-alkaline stress.*PloS one*. https://doi.org/10.1371/JOURNAL.PONE.0243112.2020
19. Li ZW,An MJ,Hong DS,et al(2022)Transcriptomic and Metabolomic Analyses Reveal the Differential Regulatory Mechanisms of Compound Material on the Responses of Brassica campestris to Saline and Alkaline Stresses. Frontiers in Plant Science. https://doi.org/10.3389/FPLS.2022.820540
20. Mashima K, Hatano M, Suzuki H,et al(2019)Identification and characterization of apigenin 6-C-glucosyltransferase involved in biosynthesis of isosaponarin in wasabi(Eutrema japonicum).Plant Cell Physiol.60(12):2733–2743.
21. Mir MA, John R, Alyemeni MN, et al(2018)Jasmonic acid ameliorates alkaline stress by improving growth performance, ascorbate glutathione cycle and glyoxylase system in maize seedlings. Sci. Rep. https://doi.org/10.1038/s41598-018-21097-3
22. Mir ZA,Ali S,Shivaraj SM,et al(2020)Genome-wide identification and characterization of chitinase gene family in Brassica juncea and Camelina sativa in response to Alternaria brassicae. Genomics.112(1):749–763.
23. Noguchi H, Yasuda Y(2007)Effect of low temperature on ethanolic fermentation in rice seedlings. J Plant Physiol.164:1013–1018.
24. Ritter A, Dittami SM, Goulitquer S,et al(2014)Transcriptomic and metabolomic analysis of copper stress acclimation in Ectocarpus siliculosus highlights signaling and tolerance mechanisms in brown algae. BMC plant biology.https://doi.org/10.1186/1471-2229-14-116
25. Sagervanshi A,Naeem A,Kaiser H,et al(2021)Early growth reduction in Vicia faba L. under alkali salt stress is mainly caused by excess bicarbonate and related to citrate and malate over accumulation. Environmental and Experimental Botany. https://doi.org/10.1016/J.ENVEXPBOT.2021.104636
26. So YY,Seong SK,Sim HJ,et al(2017)An Alcohol Dehydrogenase Gene from Synechocystis sp. Confers Salt Tolerance in Transgenic Tobacco. Frontiers in Plant Science.https://doi.org/10.3389/fpls.2017.01965
27. Sun J, He L and Li T(2019) Response of seedling growth and physiology of *Sorghum bicolor* (L.) Moench to saline-alkali stress. PLoS One. https://doi.org/10.1371/journal.pone.0220340

28. Wang WC,Pang JY,Zhang FH, et al(2021)Integrated transcriptomics and metabolomics analysis to characterize alkali stress responses in canola (Brassica napus L.). *Plant Physiology and Biochemistry*. https://doi.org/10.1016/J.PLAPHY.2021.06.021
29. Wu JX, Cao JY, Su M, et al(2019) Genome-wide comprehensive analysis of transcriptomes and small RNAs ofers insights into the molecular mechanism of alkaline stress tolerance in a citrus rootstock. Hortic Res.6:33–51.
30. Xiang G, Ma W, Gao S, et al(2019)Transcriptomic and phosphoproteomic profifiling and metabolite analyses reveal the mechanism of $NaHCO_3$-induced organic acid secretion in grapevine roots. BMC Plant Biol.https://doi.org/10.1186/s12870-019-1990-9
31. Xiong WD,Wu ZY,Liu YC,et al(2019)Mutation of 4-coumarate: Coenzyme A ligase 1 gene affects lignin biosynthesis and increases the cell wall digestibility in maize brown midrib5 mutants. Biotechnology for Biofuels.https://doi.org/10.1186/s13068-019-1421-z
32. Xu N,Liu S,Lu Z,et al(2020)Gene expression profiles and flavonoid accumulation during salt stress in Ginkgo biloba seedlings. Plants.https://doi.org/10.3390/plants9091162
33. Yan G,Shi YJ,Chen FF,et al(2022)Physiological and Metabolic Responses of Leymus chinensis Seedlings to Alkali Stress. *Plants*. https://doi.org/10.3390/PLANTS11111494
34. Zhang J,Yang DS,Li MX,et al(2016)Metabolic profiles reveal changes in wild and cultivated soybean seedling leaves under salt stress. PLoS ONE. https://doi.org/10.1371/journal.pone.0159622
35. Zhao XY, Bian XY, Li ZX, et al(2014) Genetic stability analysis of introduced *Betula pendula, Betula kirghisorum*, and *Betula pubescens* families in saline-alkali soil of northeastern China. Scand. J. For. Res. 29 (7), 639–649.
36. Zhou J,Qi AG,Wang BQ, et al(2022)Integrated Analyses of Transcriptome and Chlorophyll Fluorescence Characteristics Reveal the Mechanism Underlying Saline–Alkali Stress Tolerance in Kosteletzkya pentacarpos. Frontiers in Plant Science. https://doi.org/10.3389/fpls.2022.865572

Figures

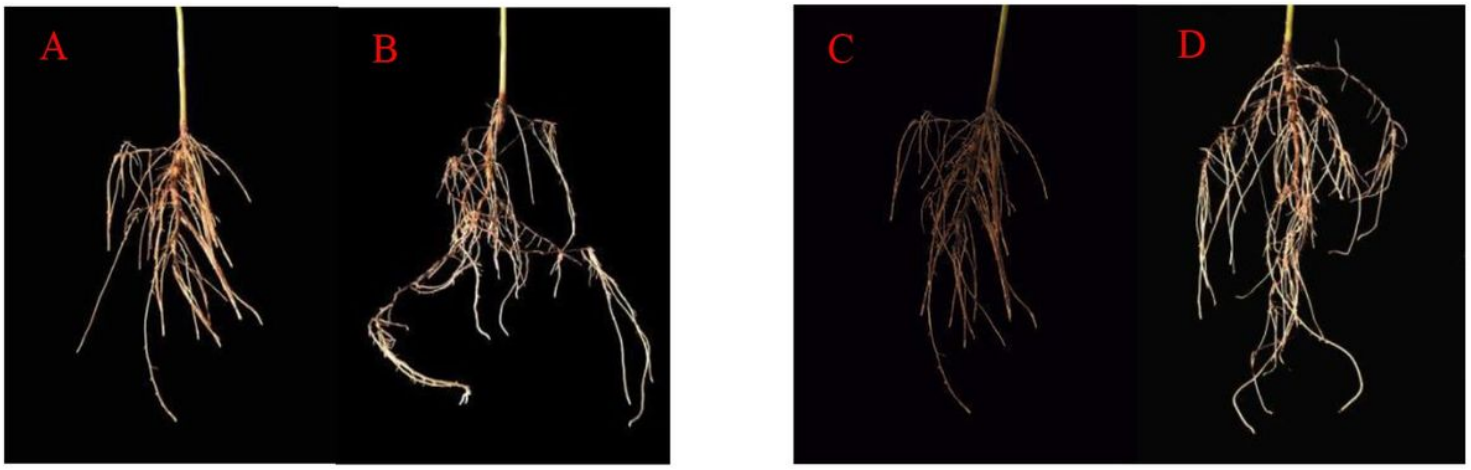

Figure 1

Roots of *Cinnamomum bodinieri* after 6h and 48h alkali stress treatment

A represents the root system (HT6) of *Cinnamomun bodinieri* after 20mmol/L Na_2CO_3 treatment for 6h B represents the root system (HCK6) of *Cinnamomun bodinieri* after 0 mmol/L Na_2CO_3 treatment for 6h C represents the root system (HT48) of *Cinnamomun bodinieri* after 20mmol/L Na_2CO_3 treatment for 48h D represents the root system (HCK48) of *Cinnamomun bodinieri* after 0 mmol/L Na_2CO_3 treatment for 48h

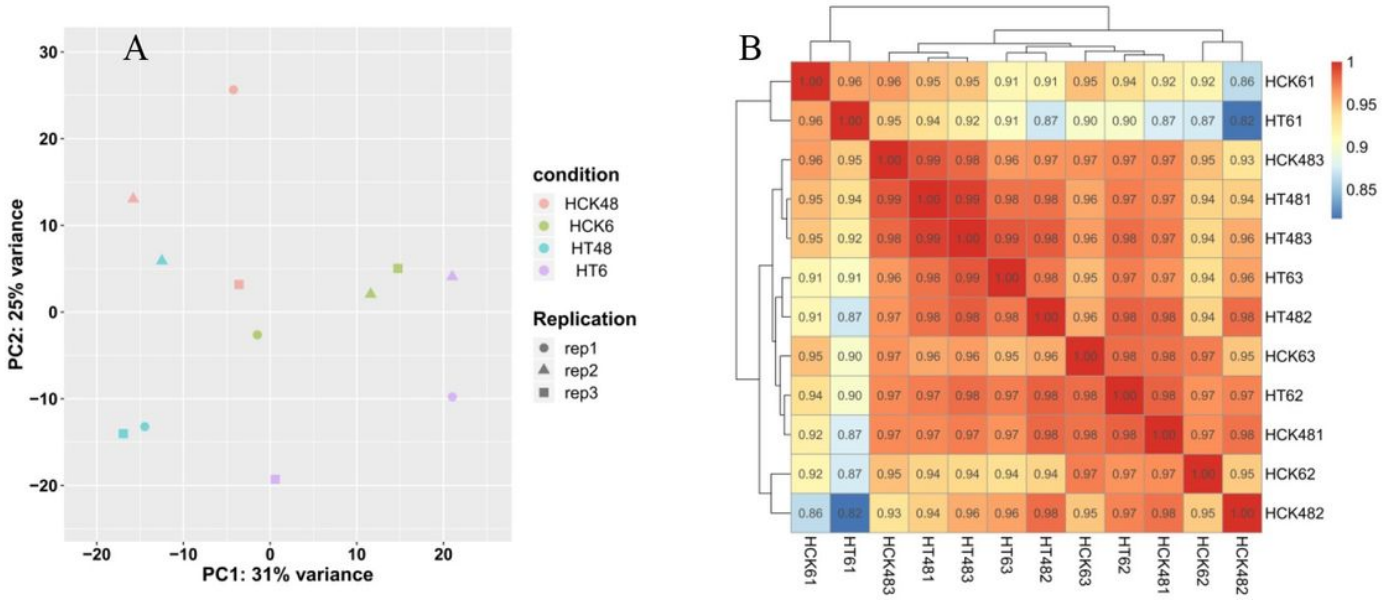

Figure 2

Quality analysis of root samples of *Cinnamomum bodinieri* after 6h and 48h alkali treatment

A represents PCA analysis; B represents sample correlation test

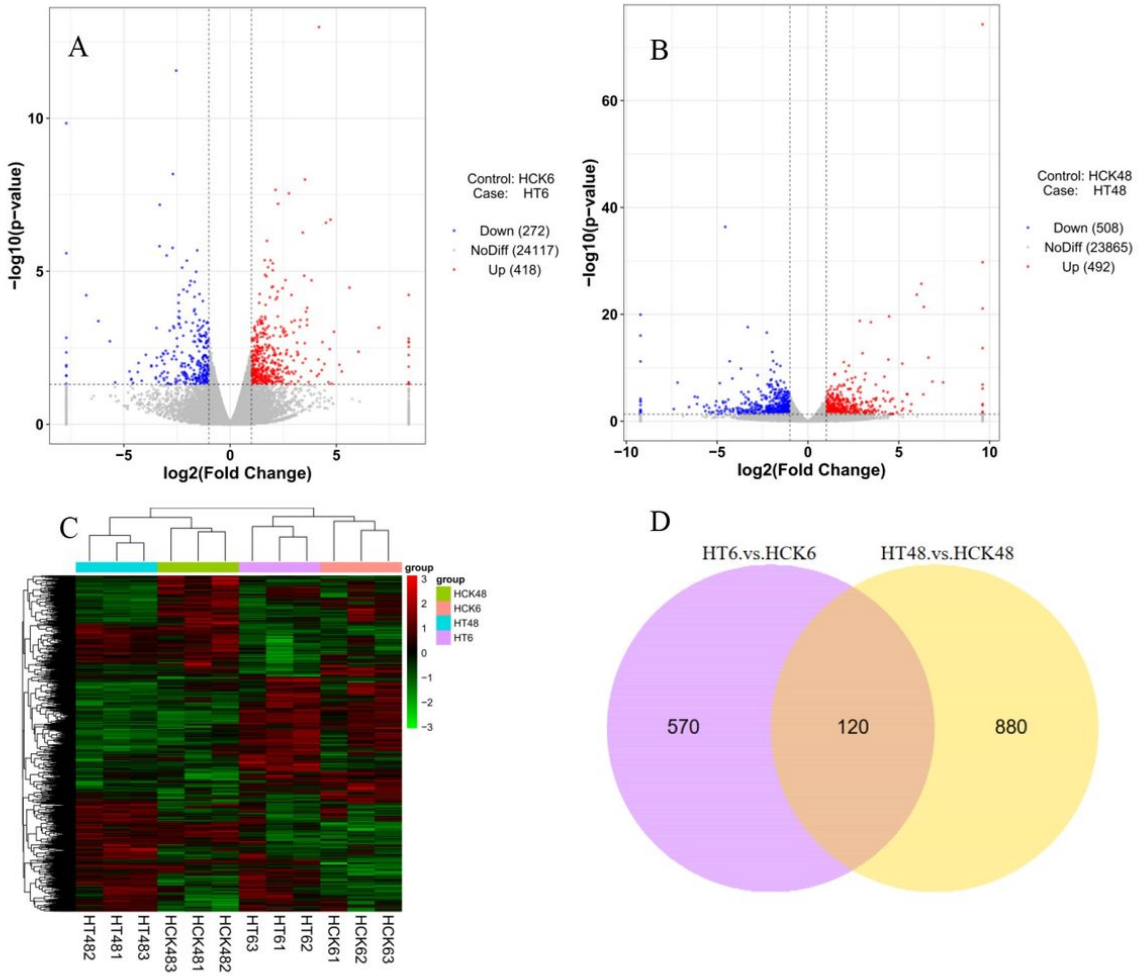

Figure 3

Change of gene expression profile of samples after 6h and 48h alkali treatment

A represents the volcanic map of gene expression of the HT6.V.HCK6 sample; B represents the volcanic map of gene expression of the HT48.V.HCK48 sample

C represents a bidirectional cluster graph (horizontal represents genes, each column is a sample, red represents highly expressed genes, green represents low expressed genes); D represents the combined Wayne diagram of HT6.V.HCK6 and HT48.V.HCK48

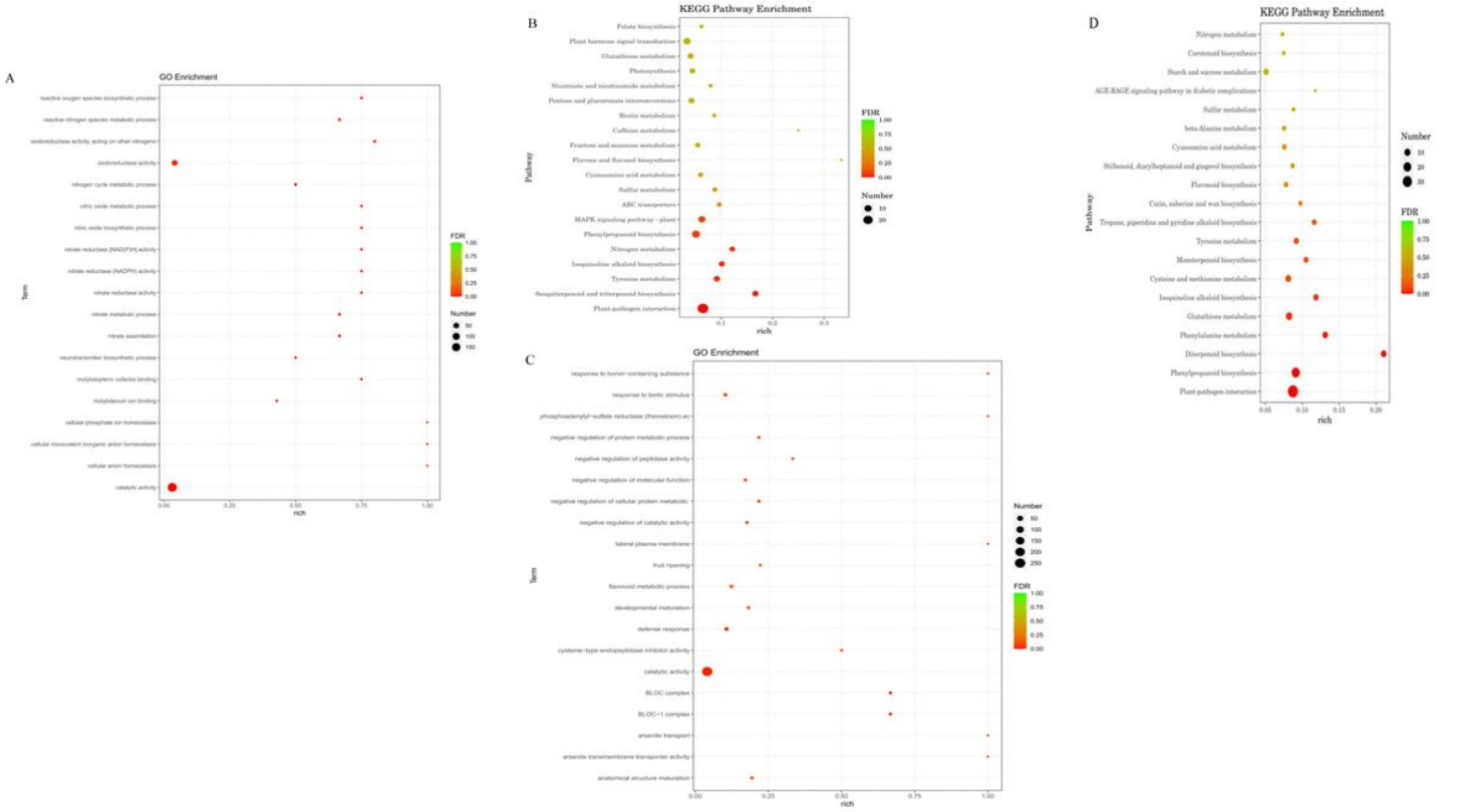

Figure 4

GO analysis and KEGG analysis of differentially expressed genes after 6h and 48h alkali treatment

A: GO analysis of differentially expressed genes in HT6.V.HCK6 combination; B: Analysis of KEGG gene differentially expressed in HT6.V.HCK6 combination

C: GO analysis of differentially expressed genes in HT48.V.HCK48 combination; D: Analysis of KEGG gene differentially expressed in HT48.V.HCK48 combination

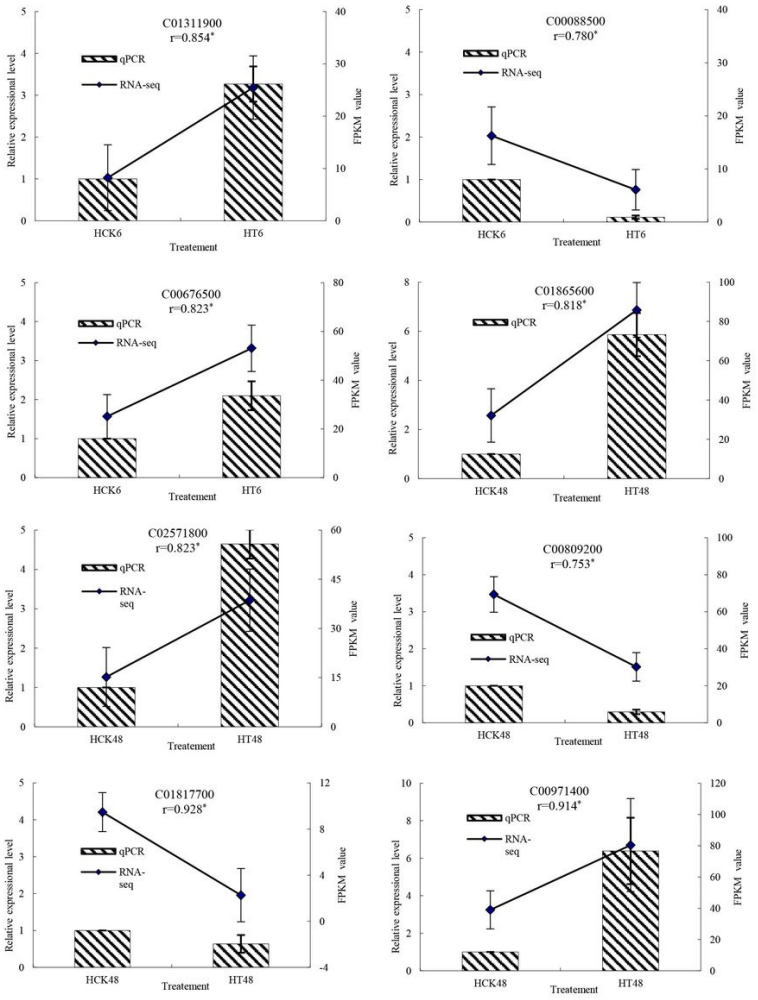

Figure 5

qPCR validation results of root transcriptome of C.*bodinieri*

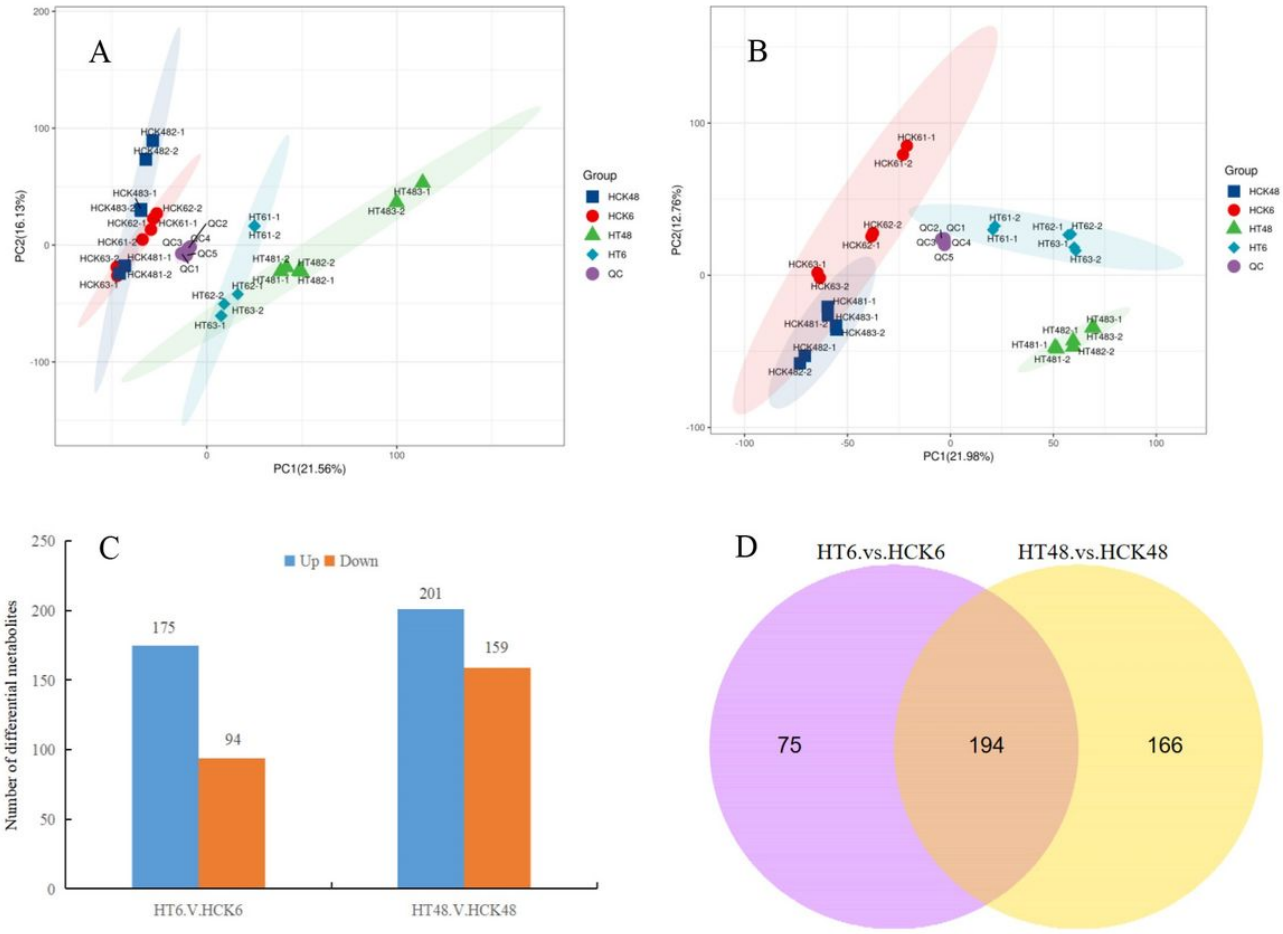

Figure 6

Screening of differentially expressed metabolites after alkali treatment for 6h and 48h

A: PCA analysis of test samples and QC samples in positive ion mode; B: PCA analysis of test samples and QC samples in negative ion mode; C: Column analysis diagram of differential expression metabolites; D: Wayne analysis diagram of differentially expressed metabolites

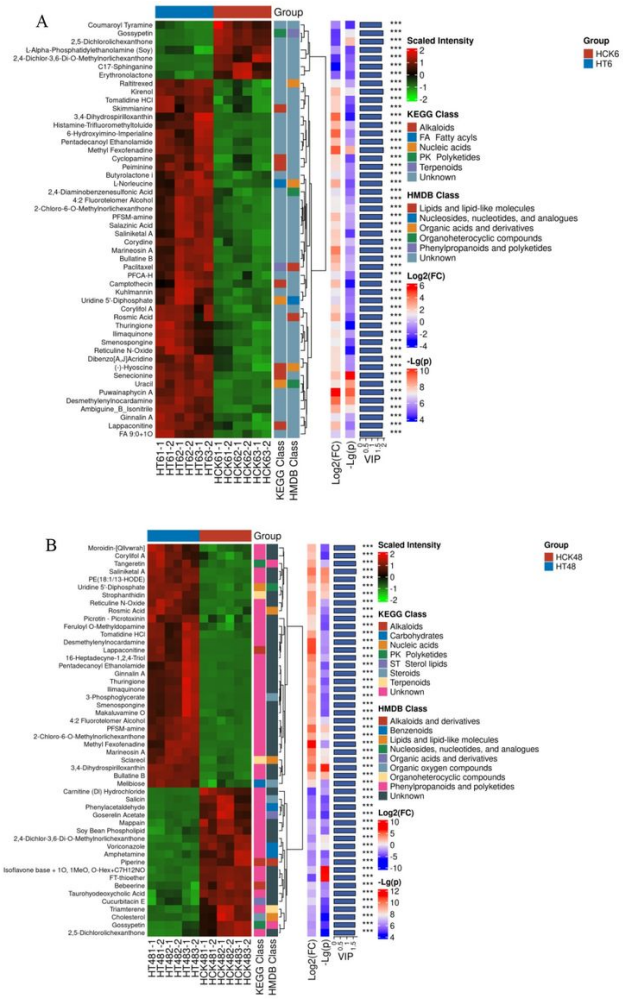

Figure 7

KEGG classification and HMDB classification of differentially expressed metabolites at 6h and 48h of alkali treatment

A: KEGG classification and HMDB classification of HT6.V.HCK6 combination differential expression metabolites; B: KEGG classification and HMDB classification of HT48.V.HCK48 combination differentially expressed metabolites

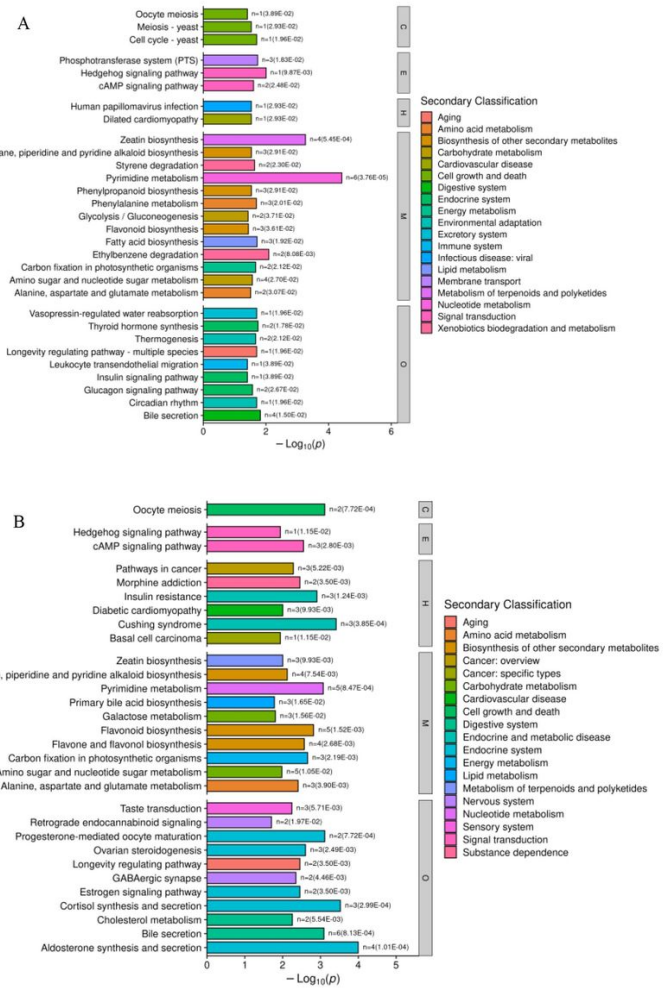

Figure 8

KEGG enrichment of differentially expressed metabolites after alkali treatment for 6h and 48h

A: KEGG enrichment of differentially expressed metabolites in HT6.V.HCK6 combination; B: KEGG enrichment of differentially expressed metabolites in HT48.V.HCK48 combinations

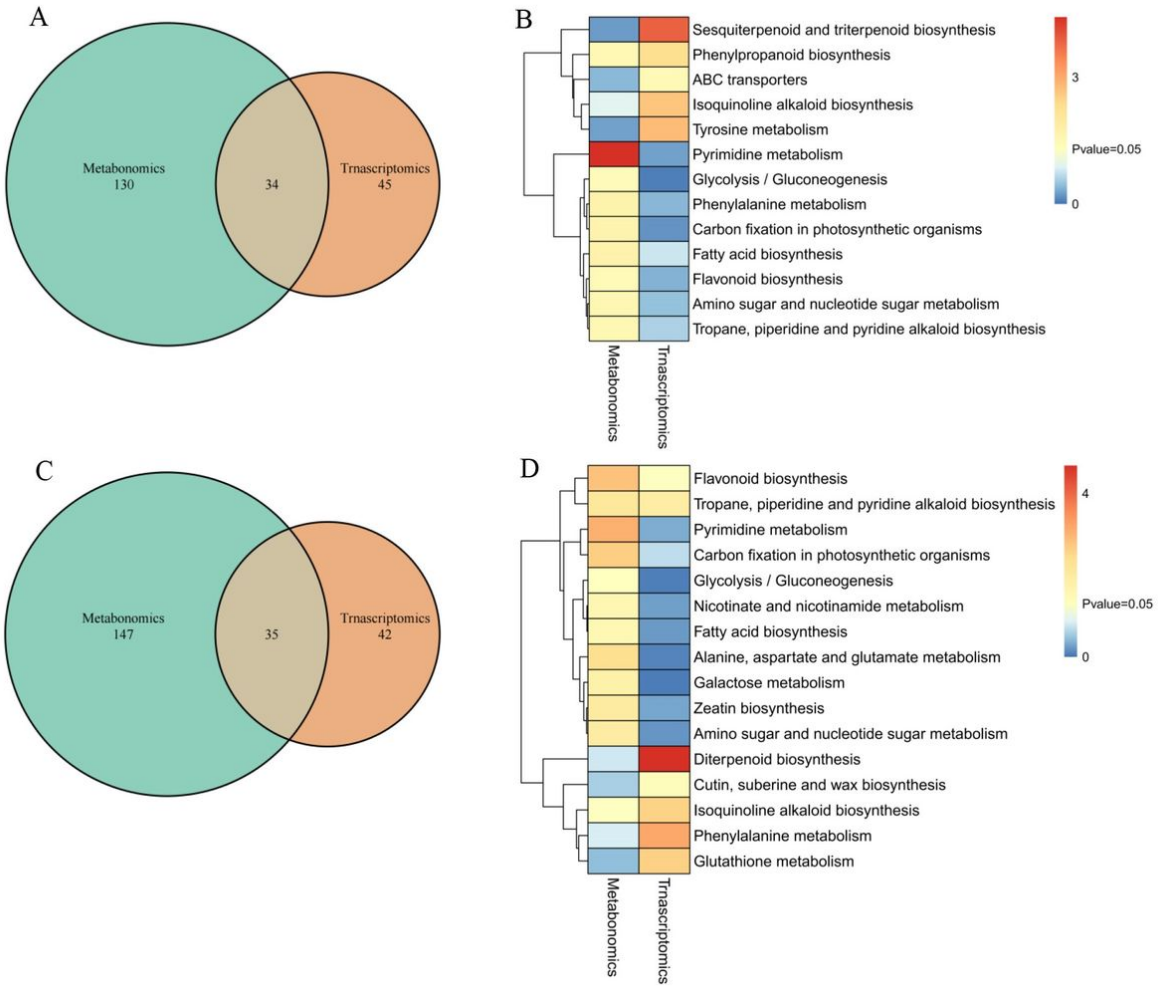

Figure 9

Joint KEGG analysis of metabolome and transcriptome

A: Combined KEGG analysis Wayne diagram of metabolome and transcriptome of HT6.V.HCK6 combination

B: Combined KEGG analysis PValue heat map of metabolome and transcriptome of HT6.V.HCK6 combination

C: Combined KEGG analysis Wayne diagram of metabolome and transcriptome of HT48.V.HCK48 combination

D: Combined KEGG analysis PValue heat map of metabolome and transcriptome of HT48.V.HCK48 combination